

## Supplementary Information

### Design and Characterization of Multi-Component Lamellar Materials Based on MWW-Type Zeolitic Layers and Metal Oxide Sub-domains

Cristina Esteban, Alexandra Velty\*, Urbano Díaz\*

Instituto de Tecnología Química, Universitat Politècnica de València, Agencia Estatal Consejo Superior de Investigaciones Científicas, 46022 Valencia, Spain

\* Corresponding Author: [udiaz@itq.upv.es](mailto:udiaz@itq.upv.es), [avelty@itq.upv.es](mailto:avelty@itq.upv.es)

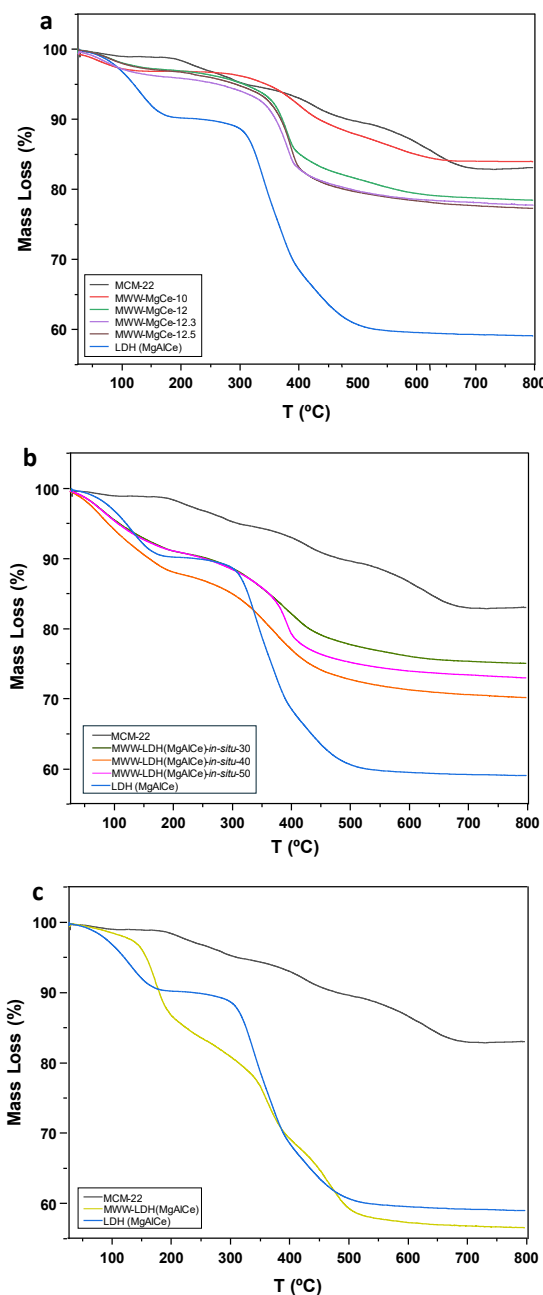


**Figure S1.** Thermogravimetric analysis (TGA). (a) As-synthesized multi-component MWW-MgCe materials obtained through method (I) at different pHs for the formation of metallic oxide sub-domains. (b) As-synthesized multi-component MWW-LDH-*in-situ* materials obtained following synthesis method (II). (c) As-synthesized multi-component MWW-LDH materials obtained following synthesis method (III).

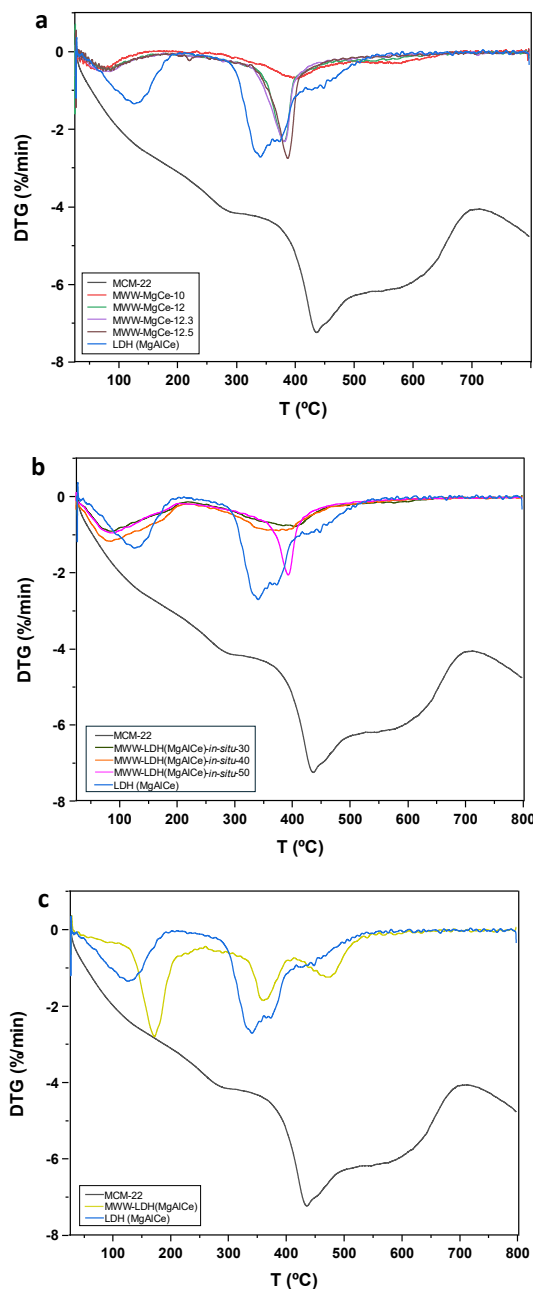


**Figure S2.** Derivative curves (DTA) from thermogravimetric analysis (TGA). (a) As-synthesized multi-component MWW-MgCe materials obtained through method (I) at different pHs for the formation of metallic oxide sub-domains. (b) As-synthesized multi-component MWW-LHD-*in-situ* materials obtained following synthesis method (II) with different LDH content. (c) As-synthesized multi-component MWW-LHD materials obtained following synthesis method (III).

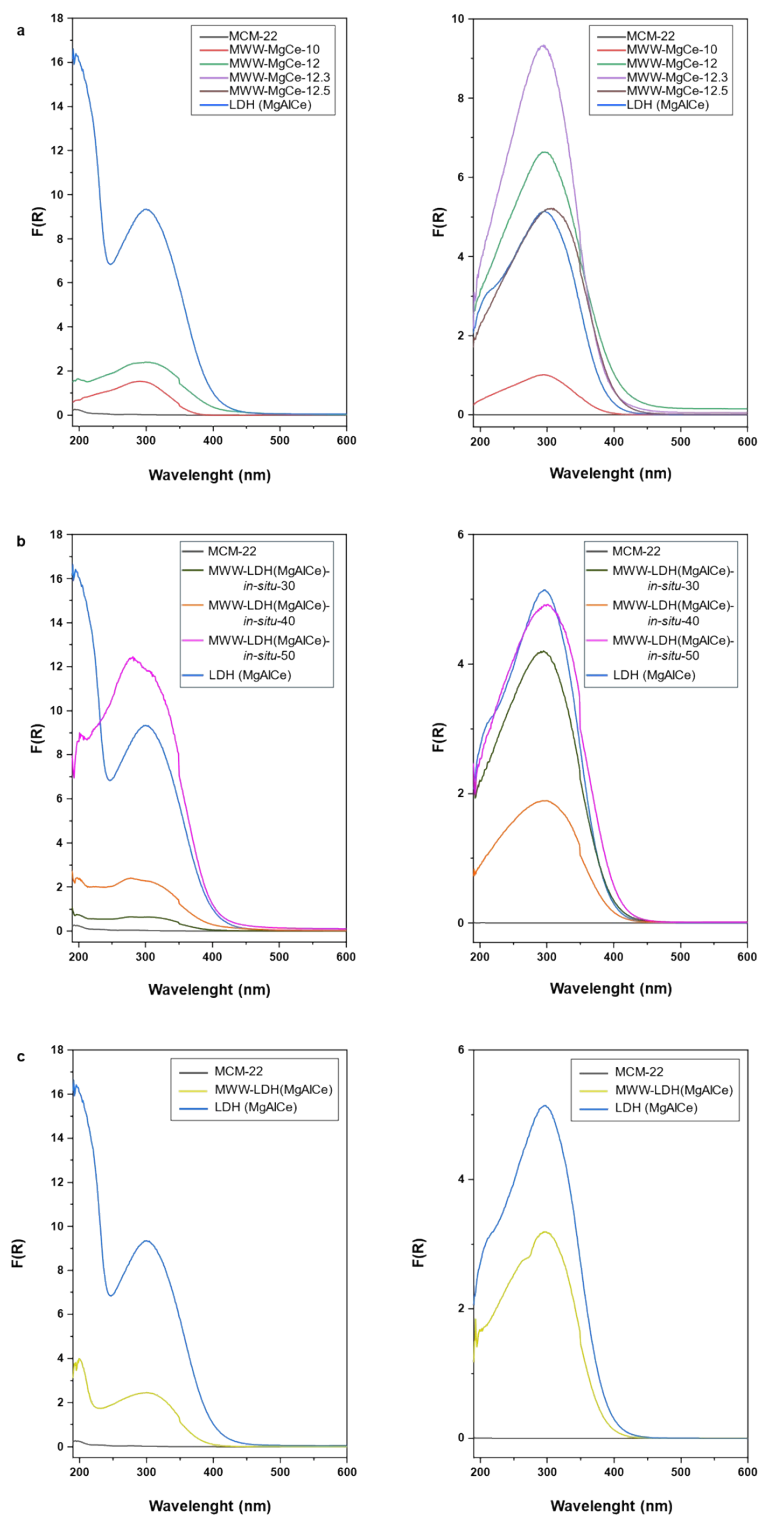


**Figure S3.** UV-Visible spectra of as-synthesized (left) and calcined (right) samples. (a) Multi-component MWW-MgCe materials obtained through method (I) at different pHs for the formation of metallic oxide sub-domains. (b) Multi-component MWW-LDH-*in-situ* materials obtained following synthesis method (II) with different LDH content. (c) Multi-component MWW-LDH materials obtained following synthesis method (III).

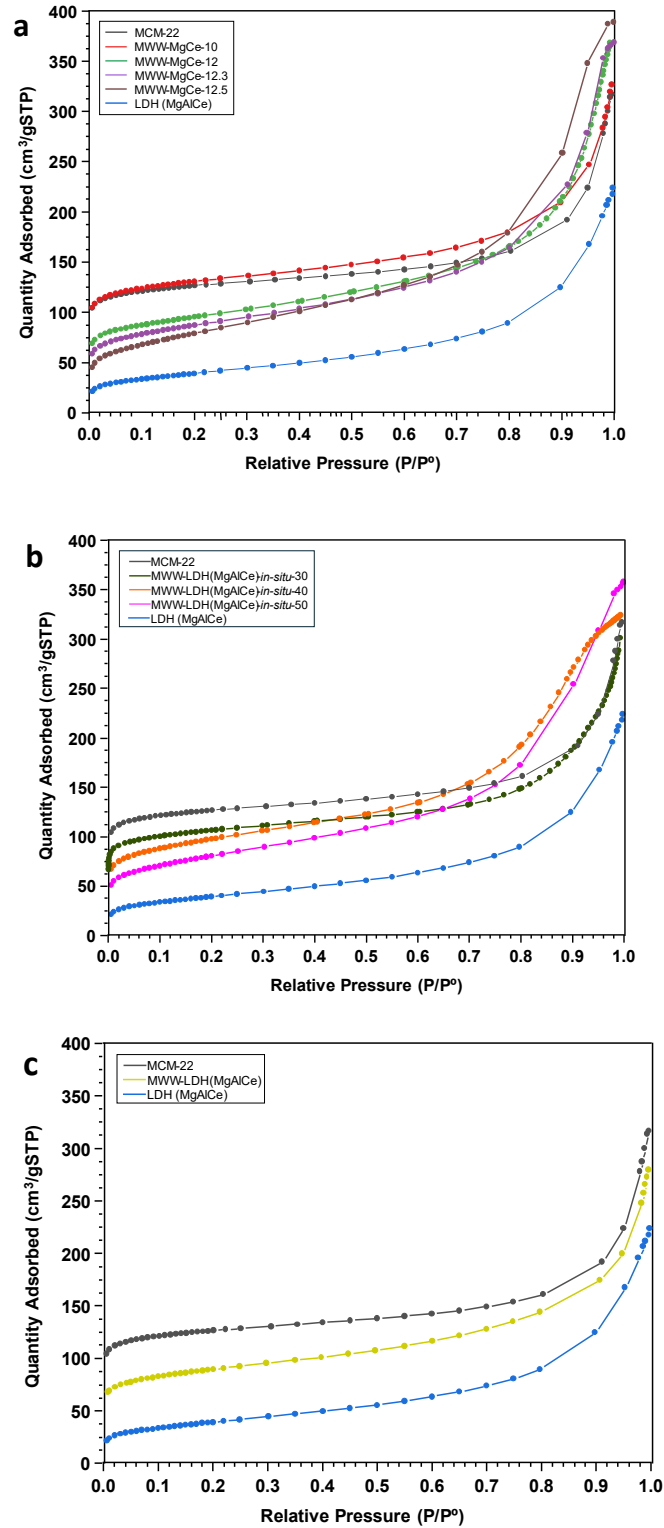


**Figure S4.** N<sub>2</sub> adsorption isotherms. (a) Multi-component MWW-MgCe materials obtained through method (I) at different pHs for the formation of metallic oxide sub-domains. (b) Multi-component MWW-LDH-*in-situ* materials obtained through method (II) with different LDH contents. (c) Multi-component MWW-LDH materials obtained following synthesis method (III).

**Table S1.** Ammonia desorbed quantity estimated from thermoprogrammed desorption analyses (TPD) of multi-component MWW-MgCe, MWW-LDH-*in-situ* and MWW-LDH materials, obtained following synthesis methods (I), (II) and (III), respectively.

<b>Material</b>	<b>Temperature (°C)<sup>1</sup></b>	<b>NH<sub>3</sub> Quantity (cm<sup>3</sup>/g)</b>
MCM-22	361	29.3
LDH (MgAlCe)	315	91.3
<i>MWW-MgCe materials</i>		
MWW-MgCe-10	204	27.8
MWW-MgCe-12	360	122.4
MWW-MgCe-12.3	399	130.3
MWW-MgCe-12.5	369	136.1
<i>MWW-in-situ materials</i>		
MWW-LDH(MgAlCe)- <i>in-situ</i> -30	336.4	60.8
MWW-LDH(MgAlCe)- <i>in-situ</i> -40	287.3	69.4
MWW-LDH(MgAlCe)- <i>in-situ</i> -50	328.0	77.9
<i>MWW-LDH materials</i>		
MWW-LDH	349.6	93.0

<sup>1</sup>Temperature of main desorption peak of the samples.

**Table S2.** Bandgap ( $E_g$ ) of the multi-component materials based on MWW layers and LDH (MgAlCe) sub-domains.

<b>Material</b>	<b><math>E_g</math> (eV)<sup>1</sup></b>
MCM-22	4.57
LDH (MgAlCe)	2.78
<i>MWW-MgCe materials</i>	
MWW-MgCe-12	2.45
<i>MWW-LHD-in-situ materials</i>	
MWW-LDH(MgAlCe)-in-situ-30	2.73
MWW-LDH(MgAlCe)-in-situ-40	2.65
MWW-LDH(MgAlCe)-in-situ-50	2.55
<i>MWW-LHD materials</i>	
MWW-LDH	2.83

<sup>1</sup>Band gap estimated using Tauc method.